



HAL
open science

Large third-order optical nonlinearity of chalcogenide glasses within gallium-tin-selenium ternary system

Feifei Chen, Jiao Zhang, Christophe Cassagne, Georges Boudebs

► **To cite this version:**

Feifei Chen, Jiao Zhang, Christophe Cassagne, Georges Boudebs. Large third-order optical nonlinearity of chalcogenide glasses within gallium-tin-selenium ternary system. *Journal of the American Ceramic Society*, 2020, 10.1111/jace.17272 . hal-02870515

HAL Id: hal-02870515

<https://univ-angers.hal.science/hal-02870515>

Submitted on 22 Feb 2024

HAL is a multi-disciplinary open access archive for the deposit and dissemination of scientific research documents, whether they are published or not. The documents may come from teaching and research institutions in France or abroad, or from public or private research centers.

L'archive ouverte pluridisciplinaire **HAL**, est destinée au dépôt et à la diffusion de documents scientifiques de niveau recherche, publiés ou non, émanant des établissements d'enseignement et de recherche français ou étrangers, des laboratoires publics ou privés.

Large third-order optical nonlinearity of chalcogenide glasses within gallium-tin-selenium ternary system

Feifei Chen^{1,2} | Jiao Zhang^{1,2} | Christophe Cassagne³ | Georges Boudebs^{3,*}

¹Laboratory of Infrared Materials and Devices, The Research Institute of Advanced Technologies, Ningbo University, Ningbo 315211, China

²Key Laboratory of Photoelectric Detection Materials and Devices of Zhejiang Province, Ningbo University, Ningbo, 315211, China

³Laboratoire de Photonique d'Angers, LPHIA, EA 4464, SFR MATRIX, UNIV Angers, 2 Boulevard Lavoisier, 49045, Angers, France

* Tel: (33) 2.41.73.54.26, Fax: (33) 2.41.73.52.16, e-mail: georges.boudebs@univ-angers.fr

ABSTRACT

We explore the third-order optical nonlinear properties of arsenic- and germanium-free chalcogenide glasses (ChGs) within a gallium-tin-selenium (Ga-Sn-Se, GSS) ternary system at wavelength of 1.064 μm in the picosecond region. A classical characterization showing the values of the absorption and the linear index will be given. Then, using D4 σ -Z-scan technique, both nonlinear refractive index (n_2) and nonlinear absorption coefficient (β) of the GSS ChGs will be measured. A comparison of the results is made with other families of chalcogenide glasses considering the figure of merit calculation. The first results show that GSS system would give better NL performance promising high potential for $n_2(\beta)$ -based photonic devices performed under clean production and green/sustainable chemistry.

Keywords: chalcogenide glasses, third-order optical nonlinearity, Z-scan.

1. INTRODUCTION

Third-order optical nonlinear (TONL) processes in chalcogenide glasses (ChGs) are much stronger than those in other optical glass systems (i.e. oxide glass and fluoride glass).¹⁻³ The main reason is provided by the existence of double lone-pair electrons in the chalcogenide elements (S, Se and Te),⁴ which could make the nonlinear photonic devices based on ChGs smaller in size and lower in energy consumption. Consequently, the TONL properties of ChGs as well as its applications for photonic devices had been intensively studied for the last decade,⁵⁻⁷ which leads to establishment of a new research field named as 'chalcogenide photonic'.⁸

Like other properties of glass materials, TONL properties of ChGs are highly composition dependent, in other word they could be adjusted on demand. The record of the maximum TONL properties were found in Te-based ChGs⁹ since Te has the largest number of bound electrons that are the easiest to be distorted by laser

irradiation. However, Te-based ChGs have band gap close to the optical communication wavelengths (1.31 μm and 1.55 μm), which make Te-based ChGs unsuitable for the present nonlinear optical devices due to the relatively high optical linear absorption. Se-based ChGs, on the other hand, have moderate TONL properties and low optical absorption at the optical communication wavelengths.¹⁰ More importantly, Se-based ChGs have large glass forming region and relatively high thermal and chemical stability. Therefore, considerable attentions had been attracted on Se-based ChGs and great potential had been expected for their applications in integrated all-optical processing devices.¹¹⁻¹³

In this work, we investigate the TONL properties of Se-based ChGs within a gallium-tin-selenium (Ga-Sn-Se, GSS) ternary system. These compositions are considered to be as completely environmental friendly and low-cost ChG system. It should also be noted that arsenic-containing compositions may act as a barrier to their development as they are considered harmful to the environment and containing an element that is considered highly toxic. By using D4 σ -Z-scan technique, both nonlinear refractive index (n_2) and nonlinear absorption coefficient (β) of the GSS ChGs are measured at 1.064 μm in the picosecond regime. We find that the GSS ChGs have relatively high TONL similar to that of the Se-based ChG families. Also, the results of the TONL dispersion (wavelength dependence) of the GSS ChGs is analyzed together with other compositions of the same Se-family and compared to a model predicting the evolution of the two-photon absorption and Kerr nonlinearity of indirect bandgap materials.

2. EXPERIMENTAL PROCEDURE

Molar composition of the GSS ChGs in this investigation as well as the corresponding label are given in Table 1. High-purity gallium (5N), tin (5N) and selenium (5N) were used as raw materials and mixed in a quartz tube which was then sealed in vacuum tube and melted in a shaking furnace. The melting temperature of the samples was set at 900 $^{\circ}\text{C}$ and maintained for 12 hours to ensure sufficient reaction of the raw materials. After that, the quartz tube was rapidly quenched into water, and the glass rod was obtained. To characterize the linear optical and TONL properties of the GSS ChGs, the glass rods were cut into plates and optically polished to thickness of 1 mm approximately. The transmission spectra of the glass samples were recorded within the range of 0.75~2.5 μm using a UV-VIS-NIR spectrophotometer (Lambda950, Perkin-Elmer, USA). Linear refractive index (n_0 at wavelength of 1.064 μm) was estimated using an infrared variable angle spectroscopy ellipsometer (IR-VASE Mark II, J.A. Woollam, USA).

The TONL properties of the GSS ChGs were characterized by D4 σ -Z-scan technique.^{14,15} The setup used to implement the measurement is presented in Fig. 1, and it is composed of a 4f-imaging system ($f_1 = f_2 = 20$ cm).

The laser source is a Nd:YAG laser delivering linearly polarized 17 ps (FWHM) single pulses at the near-infrared wavelength of 1.064 μm . Each glass sample under investigations is moved along the beam direction in the focus region, and the dimension variations in the transmitted beam profile which directly related to both the nonlinear phase-shift and the absorption is then recorded using a CCD camera. The nonlinear refractive index (n_2) is obtained from the beam waist relative variation (BWRV) spatial profile of the output beam, and the nonlinear absorption coefficient (β) is obtained from the conventional open-aperture (OA) Z-scan profile. The laser pulse energy for the measurements is set at 1.4 μJ ensuring low incident intensity to avoid any photoinduced phenomena. The main source of uncertainty comes from the calculation of the laser intensity at the focus of the lens L_1 . The estimated errors for the BWRV and the OA Z-scan measurements are 22% and 24%, respectively. All these measurements were performed at room temperature with linearly polarized light incident perpendicularly to the sample surface.

3. RESULT AND DISCUSSIONS

The transmission spectra of the GSS ChG samples are presented in Fig. 2. It can be found that the location of short-wavelength transmission edge that corresponds to the incident photon energy that would lead to electronic transitions between conduction and valence bands of the ChGs is close to 0.75 μm . The linear absorption coefficient (α) is defined by the following:

$$\alpha = \frac{\ln(T_0/T)}{l} \quad (1)$$

where T is the transmittance, T_0 is the transmittance at the baseline and l is the thickness of sample. The optical bandgap energy (E_g)^{16,17} can be estimated from the photon energy of the wavelength where α is equal to 10 cm^{-1} . E_g value of the GSS ChGs are accordingly obtained and listed in Table 1. It can be seen that the Ga content has the most significant influence on the electronic transitions in the glasses since the maximum E_g and the minimum E_g are obtained from sample with lowest Ga content (GGS1) and highest Ga content (GSS7), respectively. According to the well-established theoretical models^{18,19} showing that E_g is one of the key parameters that determine TONL properties of optical materials, element Ga that governs the E_g value could be expected to dominate the TONL properties of the GSS ChGs.

The TONL properties including nonlinear refraction (NR) and nonlinear absorption (NA) behavior of the GSS ChGs is investigated by D4 σ -Z-scan at wavelength of 1.064 μm . Firstly, the NR behavior of the GSS samples is characterized by BWRV measurements, and an example obtained from sample GSS1 is shown in Fig. 3(a). Configuration of the BWRV curve illustrates that the transmitted light beam through the sample exhibits a focusing behavior with a widening beam (peak) at the pre-focus and a narrowing beam (valley) behavior at the post-focus

positions. This behavior, in contrast to the classical signature of Z-scan, definitely indicates the positive sign of the nonlinear refractive index (n_2) at the testing wavelength of 1.064 μm . By fitting the BWRV curve (as described in Ref. 14), n_2 value of the GSS ChGs were estimated and normalized to the silica one (based on $n_2(\text{SiO}_2) \approx 2.6 \times 10^{-20} \text{ m}^2/\text{W}$).²⁰ As it can be seen by the measured data given in Table 1, the maximum n_2 value (2912 times that of the silica) is obtained from GSS7 with the highest Ga content and its n_2 is over 50% higher than that of the minimum obtained from GSS1 with the lowest Ga content. Compared to other Se-based ChGs²¹⁻²³ with high n_2 as given in Table 1, the n_2 value of the present GSS ChGs is the highest and the maximum n_2 is over two times that of $\text{As}_{40}\text{Se}_{60}$ known to have the record of the maximal n_2 (absolute value is $3.0 \times 10^{-17} \text{ m}^2/\text{W}$ at 1.25 μm) among the Se-based ChGs.^{10,21-24}

Secondly, the NA behavior of the GSS ChGs is investigated by the classical open-aperture (OA) Z-scan measurement. Fig. 3(b) gives an example of the normalized transmittance for GSS1. It is clear that there is a transmittance decrease when the sample is moving close to the focus point ($Z = 0$), indicating the presence of a nonlinear absorption phenomenon at 1.064 μm . Since the value of the normalized photon energy ($h\nu/E_g$, the photon energy $h\nu$ is 1.17 eV at 1.064 μm) of the present GSS ChGs is between 0.71 and 0.78, therefore it is above half E_g , the NA signal can be attributed to two-photon absorption (TPA). The related β coefficient can be estimated by fitting the OA Z-scan with the well-established TPA model.²⁵ According to the obtained β values presented in Table 1, it can be seen that the maximum is also found for sample GSS7. All the β values of the GSS ChGs are larger than those of other Se-based ChGs, which means that two-photon resonant enhancement accompanied by TPA could be a significant contribution to the large NR behavior of the GSS ChGs.

According to the above calculated TONL parameters of the GSS ChGs, two figure of merits that usually are used to evaluate the trade-off between nonlinear refraction, linear absorption and nonlinear absorption of the propagating light:²⁶

$$W = \frac{n_2 I_0}{\alpha \lambda} \quad (2)$$

$$T = \frac{n_2}{\beta \lambda} \quad (3)$$

where λ is the testing wavelength of 1.064 μm , I_0 is the laser intensity at the lens focus. For the first FOM (W) as given in Table 1, all the present GSS ChGs satisfied the criterion of $W > 1$ that is required for materials to be applied in nonlinear optical waveguide devices. So, the magnitude of the nonlinear refraction in the GSS ChGs is sufficient to overcome the optical losses from linear absorption for practical use. However, for the second FOM (T), all the GSS ChGs did not validate the criterion of $T > 1$ due to the presence of strong TPA at 1.064 μm . Since

the TPA dispersion (wavelength dependence) of ChGs is generally in accordance with semiconductors,²⁷ we can expect reduced TPA of the GSS ChGs at longer wavelengths due to lower $h\nu/E_g$, especially at 1.55 μm ($h\nu = 0.8$ eV). If this is the case, $h\nu/E_g$ of the GSS ChGs would be more close to the obtained empirical maximum (at $h\nu/E_g = 0.45$) for both of T and n_2 values.²²

As mentioned above, TONL dispersion of ChGs can be theoretically predicted by the well-established models developed for direct¹⁸ and indirect¹⁹ bandgap semiconductors. Since all the previous work^{23,27,28} were done by Ge- and As-based ChGs, it is hence important to further verify these models by using the TONL parameters of the GSS specimen that are without Ge and As incorporation. First of all, the dispersion model developed by Dinu¹⁹ for indirect bandgap semiconductors is more appropriate for the present GSS ChGs than the model developed for direct bandgap semiconductors, because the later predicts negative n_2 at $h\nu/E_g > 0.7$.¹⁸ According to the Eqs. (13) and (16) in Ref. 19, the curves of normalized n_2 and β values as a function of $h\nu/E_g$ are plotted, and the comparison with the measured values from the present GSS ChGs and other ChGs in previous studies^{21-23,29,30} is done after shifting vertically the theoretical curves to fit the experimental data. This way informs on the good general trend relative to the evolution of the parameters as a function of the normalized photon energy. The experimental data and the theoretical curves are shown in Fig. 4, where it can be seen that the dispersion of both n_2 and β values are generally in good agreement. The theoretical evolutions in Dinu's model, indicate that the TPA induced electron transitions between conduction and valence bands of ChGs could be phonon-assisted. The largest deviation (by a factor of 1.6 larger) between experimental and theoretical n_2 value of the GSS ChGs occurred in sample GSS7 with highest $h\nu/E_g$ value of 0.768, that's because the mathematical expression for dispersion of n_2 given in Ref. 19 is derived from degenerate TPA for simplicity, which will lead to progressive decrease of prediction accuracy when $h\nu/E_g$ is high above 0.5. Nevertheless, since Dinu considered the model being an order-of-magnitude estimate due to the drastic approximations and uncertainties in the values of the physical parameters, the maximum deviation factor of 1.6 is quite acceptable. It will be a more delicate work to modify this model to specific ChGs according to their precise physical parameters, which is highly useful for the design of nonlinear optical devices based on ChGs.

4. CONCLUSIONS

In summary, we have presented the third-order optical nonlinearity of chalcogenide glasses within a gallium-tin-selenium (Ga-Sn-Se) ternary system, which is a completely environment friendly and low-cost ChG system. By employing the D4 σ -Z-scan technique, both nonlinear refraction and nonlinear absorption behavior of the glasses were characterized in the near-infrared at 1.064 μm in the picosecond regime. The nonlinear refractive

index (n_2) of the Ga-Sn-Se glasses is much larger than those of glasses in other Se-based systems reported previously. The maximum n_2 value is obtained from glass with highest Ga content, and the value is 2912 times higher than that of the fused silica. The Ga-Sn-Se glasses show two-photon absorption at 1.064 μm , and the corresponding two-photon absorption coefficient (β) which is at least 8.5 cm/GW is unfortunately too high for these glasses to be applied in all-optical processing devices, but relief of such situation is expected at longer wavelengths in which the two-photon absorption would significantly be reduced. The use of these glasses for optical limiting applications may be a more judicious choice. The general dispersion (wavelength dependence) of the TONL parameters (n_2 and β) of the Ga-Sn-Se glasses is in qualitative agreement with theoretical model developed based on indirect bandgap semiconductors.

ACKNOWLEDGEMENTS

This work was partially supported by the National Key Research and Development Program of China (grant no. 2016YFB0303803), National Natural Science Foundation of China (grant no. 61675106) and Natural Science Foundation of Zhejiang Province (grant no. LY19F050005). It was also sponsored by K.C. Wong Magna Fund in Ningbo University.

REFERENCES

1. J. L. Adam, X. Zhang, Chalcogenide glasses: preparation, properties and applications, Woodhead Publishing Limited, Sawston, Cambridge, 2013.
2. D. W. Hall, M. A. Newhouse, N. F. Borrelli, W. H. Dumbaugh, and D. L. Weidman, "Nonlinear optical susceptibilities of high-index glasses," *Applied Physics Letters*, 54[14] 1293-95 (1989).
3. H. Nasu, Y. Ibara, and K. i. Kubodera, "Optical third-harmonic generation from some high-index glasses," *Journal of Non-Crystalline Solids*, 110[2] 229-34 (1989).
4. L. Petit, N. Carlie, K. Richardson, A. Humeau, S. Cherukulappurath, and G. Boudebs, "Nonlinear optical properties of glasses in the system Ge/Ga-Sb-S/Se," *Optical Letters*, 31[10] 1495-97 (2006).
5. L. Li, H. Lin, S. Qiao, Y. Zou, S. Danto, K. Richardson, J. D. Musgraves, N. Lu, and J. Hu, "Integrated flexible chalcogenide glass photonic devices," *Nature Photonics*, 8[8] 643-49 (2014).
6. C. R. Petersen, U. Møller, I. Kubat, B. Zhou, S. Dupont, J. Ramsay, T. Benson, S. Sujecki, N. Abdel-Moneim, Z. Tang, D. Furniss, A. Seddon, and O. Bang, "Mid-infrared supercontinuum covering the 1.4–13.3 μm molecular fingerprint region using ultra-high NA chalcogenide step-index fibre," *Nature Photonics*, 8[11] 830-34 (2014).

7. V. Mittal, M. Nedeljkovic, D. J. Rowe, G. S. Murugan, and J. S. Wilkinson, "Chalcogenide glass waveguides with paper-based fluidics for mid-infrared absorption spectroscopy," *Optical Letters*, 43[12] 2913-16 (2018).
8. B. J. Eggleton, B. Luther-Davies, and K. Richardson, "Chalcogenide photonics," *Nature Photonics*, 5[3] 141-48 (2011).
9. S. Cherukulappurath, M. Guignard, C. Marchand, F. Smektala, and G. Boudebs, "Linear and nonlinear optical characterization of tellurium based chalcogenide glasses," *Optics Communications*, 242[1] 313-19 (2004).
10. G. Lenz, J. Zimmermann, T. Katsufuji, M. E. Lines, H. Y. Hwang, S. Spälter, R. E. Slusher, S. W. Cheong, J. S. Sanghera, and I. D. Aggarwal, "Large Kerr effect in bulk Se-based chalcogenide glasses," *Optical Letters*, 25[4] 254-56 (2000).
11. J. M. Morris, M. D. Mackenzie, C. R. Petersen, G. Demetriou, A. K. Kar, O. Bang, and H. T. Bookey, "Ge₂₂As₂₀Se₅₈ glass ultrafast laser inscribed waveguides for mid-IR integrated optics," *Optical Materials Express*, 8[4] 1001-11 (2018).
12. M. R. Krogstad, S. Ahn, W. Park, and J. T. Gopinath, "Nonlinear characterization of Ge₂₈Sb₁₂Se₆₀ bulk and waveguide devices," *Opt. Express*, 23[6] 7870-78 (2015).
13. T. Kuriakose, E. Baudet, T. Halenkovič, M. M. R. Elsayy, P. Němec, V. Nazabal, G. Renversez, and M. Chauvet, "Measurement of ultrafast optical Kerr effect of Ge–Sb–Se chalcogenide slab waveguides by the beam self-trapping technique," *Optics Communications*, 403 352-57 (2017).
14. G. Boudebs, V. Besse, C. Cassagne, H. Leblond, and C. B. de Araújo, "Nonlinear characterization of materials using the D4σ method inside a Z-scan 4f-system," *Optical Letters*, 38[13] 2206-08 (2013).
15. C. B. de Araújo, A. S. L. Gomes, and G. Boudebs, "Techniques for nonlinear optical characterization of materials: a review," *Reports on Progress in Physics*, 79[3] 036401 (2016).
16. C. Quémard, F. Smektala, V. Couderc, A. Barthélémy, and J. Lucas, "Chalcogenide glasses with high nonlinear optical properties for telecommunications," *Journal of Physics and Chemistry of Solids*, 62[8] 1435-40 (2001).
17. F. Smektala, C. Quémard, V. Couderc, and A. Barthélémy, "Non-linear optical properties of chalcogenide glasses measured by Z-scan," *Journal of Non-Crystalline Solids*, 274[1] 232-37 (2000).
18. M. Sheik-Bahae, D. C. Hutchings, D. J. Hagan, and E. W. V. Stryland, "Dispersion of bound electron nonlinear refraction in solids," *IEEE Journal of Quantum Electronics*, 27[6] 1296-309 (1991).
19. M. Dinu, "Dispersion of phonon-assisted nonresonant third-order nonlinearities," *IEEE Journal of Quantum Electronics*, 39[11] 1498-503 (2003).

20. D. Milam, "Review and assessment of measured values of the nonlinear refractive-index coefficient of fused silica," *Applied Optics*, 37[3] 546-50 (1998).
21. J. M. Harbold, F. Ö. Ilday, F. W. Wise, J. S. Sanghera, V. Q. Nguyen, L. B. Shaw, and I. D. Aggarwal, "Highly nonlinear As–S–Se glasses for all-optical switching," *Optical Letters*, 27[2] 119-21 (2002).
22. J. M. Harbold, F. O. Ilday, F. W. Wise, and B. G. Aitken, "Highly nonlinear Ge-As-Se and Ge-As-S-Se glasses for all-optical switching," *IEEE Photonics Technology Letters*, 14[6] 822-24 (2002).
23. T. Wang, X. Gai, W. Wei, R. Wang, Z. Yang, X. Shen, S. Madden, and B. Luther-Davies, "Systematic z-scan measurements of the third order nonlinearity of chalcogenide glasses," *Optical Materials Express*, 4[5] 1011-22 (2014).
24. T. Kuriakose, E. Baudet, T. Halenkovič, M. M. R. Elsayy, P. Němec, V. Nazabal, G. Renversez, and M. Chauvet, "Measurement of ultrafast optical Kerr effect of Ge–Sb–Se chalcogenide slab waveguides by the beam self-trapping technique," *Optics Communications*, 403 352-57 (2017).
25. M. Sheik-Bahae, A. A. Said, T. Wei, D. J. Hagan, and E. W. V. Stryland, "Sensitive measurement of optical nonlinearities using a single beam," *IEEE Journal of Quantum Electronics*, 26[4] 760-69 (1990).
26. D. Marchese, M. De Sario, A. Jha, A. K. Kar, and E. C. Smith, "Highly nonlinear GeS₂-based chalcogenide glass for all-optical twin-core-fiber switching," *Journal of the Optical Society of America B*, 15[9] 2361-70 (1998).
27. K. Tanaka, "Nonlinear optics in glasses: How can we analyze?," *Journal of Physics and Chemistry of Solids*, 68[5] 896-900 (2007).
28. A. Prasad, C.-J. Zha, R.-P. Wang, A. Smith, S. Madden, and B. Luther-Davies, "Properties of Ge_xAs_ySe_{1-x-y} glasses for all-optical signal processing," *Optics Express*, 16[4] 2804-15 (2008).
29. J. Troles, F. Smektala, G. Boudebs, A. Monteil, B. Bureau, and J. Lucas, "Chalcogenide glasses as solid state optical limiters at 1.064 μm," *Optical Materials*, 25[2] 231-37 (2004).
30. T. Sun, X. Xue, Y. Yang, C. Lin, S. Dai, X. Zhang, W. Ji, and F. Chen, "Correlating structure with third-order optical nonlinearity of chalcogenide glasses within a germanium–sulfur binary system," *Journal of Non-Crystalline Solids*, 522 119562 (2019).

Table 1. Compositions, linear refractive index (n_0), optical bandgap energy (E_g), TONL parameters (n_2 , β , W and T) of the GSS ChGs and other Se-based ChGs previous reports for reference.

sample	Composition (in mol%)	n_0 ± 0.04	E_{opg} (eV) ± 0.03	n_2 (times to SiO ₂) $\pm 24\%$	β (cm/GW) $\pm 22\%$	W $\pm 40\%$	T $\pm 46\%$
GSS1	Ga ₃ Sn ₂₀ Se ₇₅	2.59	1.62	1924	13.0	5.2	0.42
GSS2	Ga ₁₀ Sn ₁₆ Se ₇₄	2.56	1.61	2475	8.5	2.2	0.82
GSS3	Ga ₁₀ Sn _{17.5} Se _{72.5}	2.60	1.63	2049	10.4	3.4	0.56
GSS4	Ga ₁₀ Sn _{18.5} Se _{71.5}	2.61	1.59	2163	10.4	3.5	0.59
GSS5	Ga ₁₀ Sn ₂₀ Se ₇₀	2.65	1.58	2491	11.4	2.8	0.61
GSS6	Ga ₁₀ Sn _{22.5} Se _{67.5}	2.61	1.56	1971	9.9	2.6	0.56
GSS7	Ga ₁₅ Sn ₂₀ Se ₆₅	2.65	1.53	2912	15.6	1.5	0.53
	*As ₄₀ Se ₆₀ in Ref. 21	2.81	1.77	1200	2.8	-	1
	*Ge ₂₀ As ₄₀ Se ₄₀ in Ref. 22	-	1.83	880	2.8	-	0.63
	*Ge _{12.5} Sb ₂₀ Se _{67.5} in Ref. 23	2.80	1.57	438	0.37	-	0.2
	*Ge ₁₅ Sb ₁₀ Se ₇₅ in Ref. 23	2.60	1.72	288	-	-	>52

*TONL parameters (n_2 , β and T) in Refs. 21 and 22 are measured at 1.25 μm , in Ref. 23 are measured at 1.55 μm .

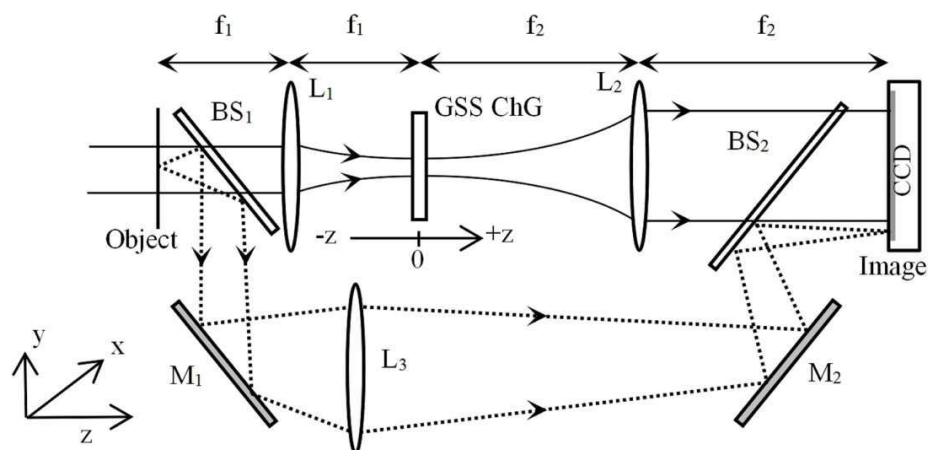


Fig. 1. Experimental D4σ-Z-scan setup. The GSS ChG sample is scanned along the beam direction around the focal plane ($z=0$). The labels refer to: lenses (L1, L2 and L3), beam splitters (BS1 and BS2), mirrors (M1 and M2), Camera (CCD).

169x78mm (300 x 300 DPI)

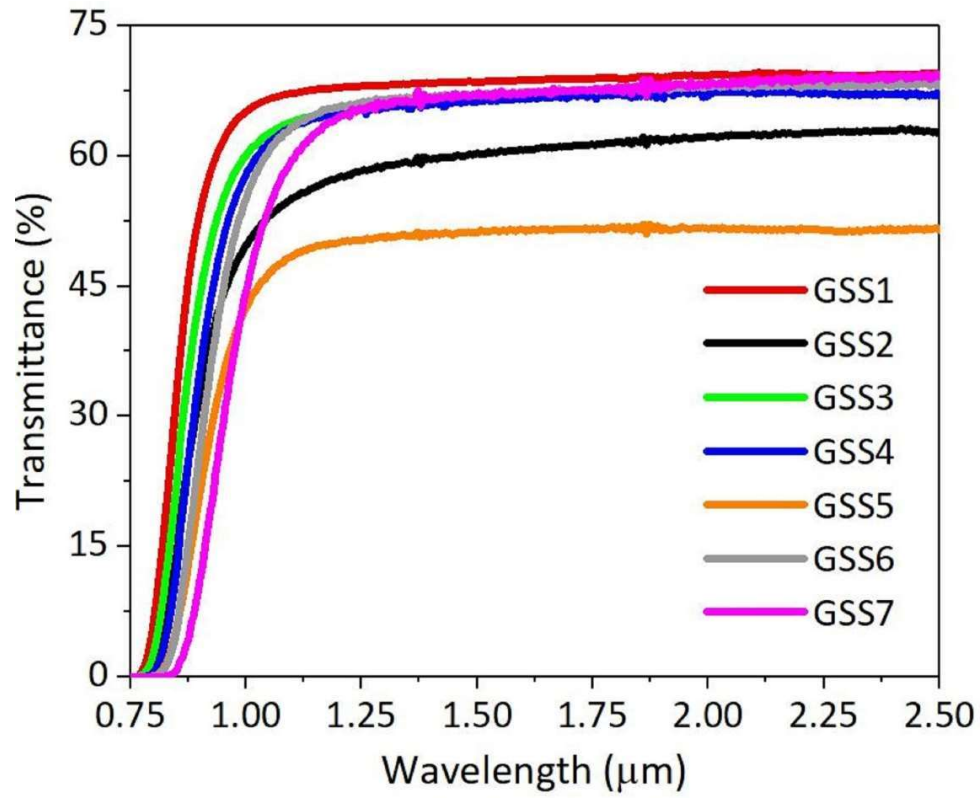


Fig. 2. Transmission spectra of the GSS ChGs.

169x140mm (300 x 300 DPI)

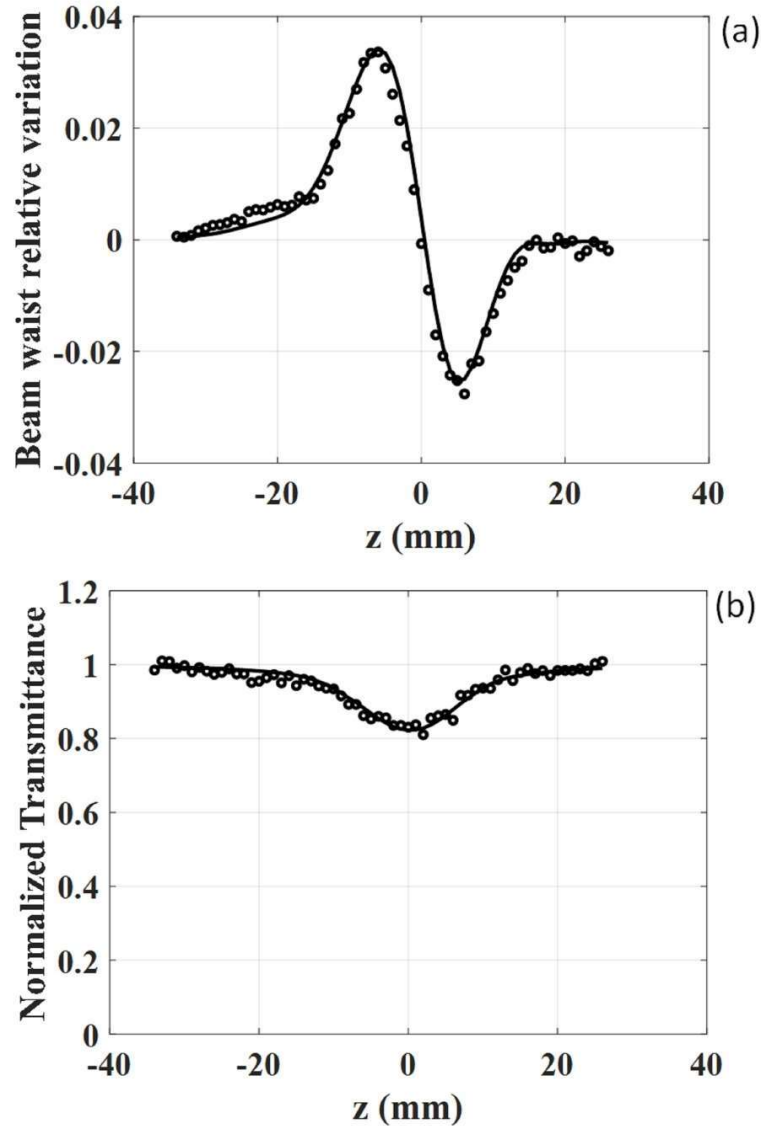


Fig. 3. (a) Beam waist relative variation curve and (b) open-aperture Z-scan curve of sample GSS1. The solid lines are the numerical fitting.

169x257mm (300 x 300 DPI)

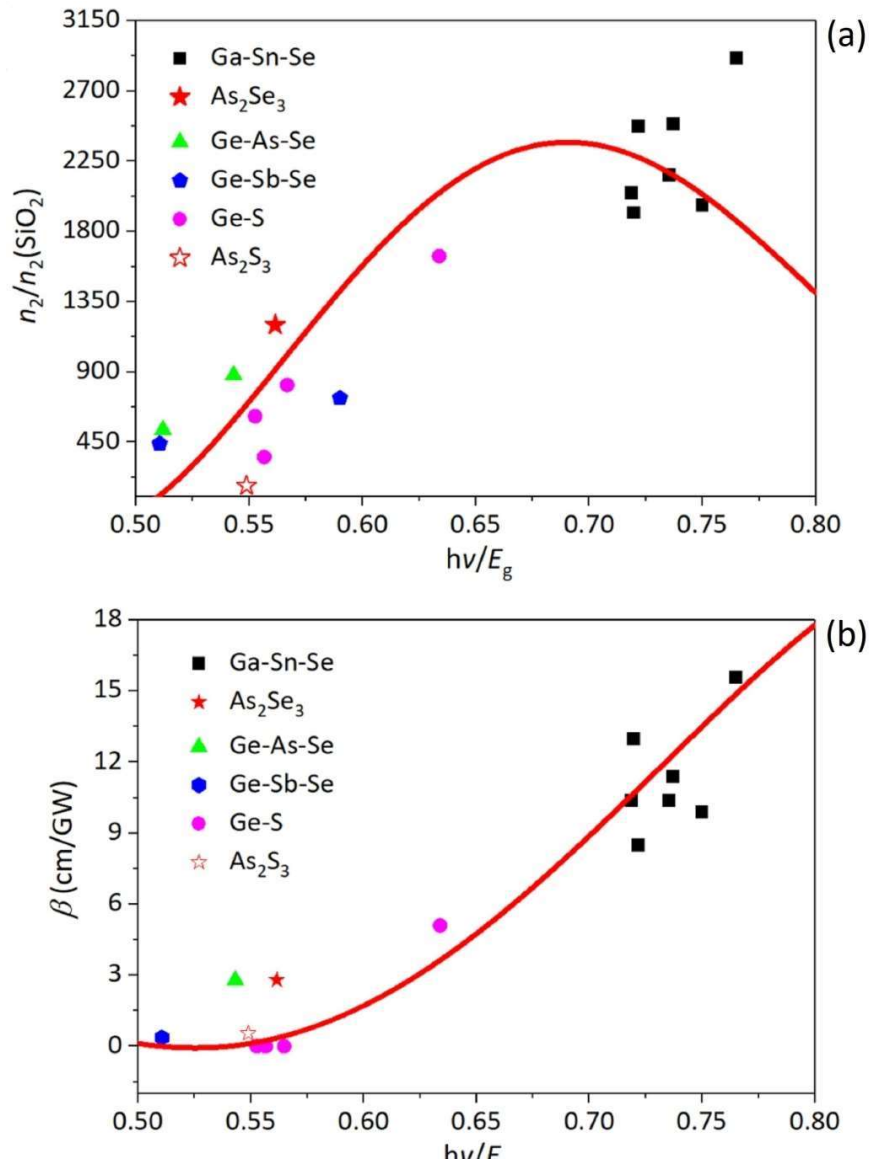


Fig. 4. (a) n_2 and (b) β values of the present GSS ChGs together with the previously reported values from ChGs in Ge-As-Se measured at 1.25 μm in Ref. 22, Ge-Sb-Se measured at 1.55 μm in Ref. 23, As_2S_3 measured at 1.064 μm in Ref. 29, As_2Se_3 measured at 1.25 μm in Ref. 21 and Ge-S measured at 0.8 μm in Ref. 30 as a function of $h\nu/E_g$. The solid line is the fitting according to Dinu's model for indirect bandgap semiconductors.

174x230mm (300 x 300 DPI)